The Impacts of East China Sea Kuroshio Front on Winter Heavy Precipitation Events in Southern China

HaoKun Bai[*], HaiBo Hu[*,#], Xuejuan Ren[*], Xiu-Qun Yang[*], Yang Zhang[*], Kefeng Mao[2], Yihang Zhao[*]

[*] CMA-NJU Joint Laboratory for Climate Prediction Studies, Instituted for Climate and Global Change Research, School of Atmospheric Science, Nanjing University, Nanjing 210093, China

2 National University of Defense Technology

#Corresponding author: H.-B. Hu (huhaibo@nju.edu.cn)

Key Points:

- The high-frequency wind-coupled-precipitation events over East China Sea contribute more than half winter heavy-rainy days in Southern China.
- The water vapor sources of winter heavy precipitation in Southern China are observed cross boundary layer from warm flank of Kuroshio front.
- The low-temperature-precipitation disaster in Southern China in 2008 winter are connected with the special aforementioned events.

Abstract

The wintertime Kuroshio sea surface temperature (SST) front have the significant climate effects on southern China. The study demonstrates a close relationship between heavy precipitation over Southern China and Kuroshio SST front in winter. More than half winter heavy rainfall events in Southern China are proved to be resulted from strong High-frequency Variability events of the sea surface Wind Coupled with Precipitation (HV-WCP) over Kuroshio SST front. One day before strong HV-WCP events, the initial precipitation appears over Middle-lower Yangtze River due to the significantly enhanced frontal intensity. Then the precipitation generates low level cyclone and southeasterly wind anomalies, after it moving into Kuroshio front area because of the winter monsoon. The significant marine atmospheric boundary layer (MABL) height gradient over Kuroshio leads to plentiful moisture transporting from MABL into free atmosphere and enhances the local precipitation again. This process further causes the large-scale stratus rainband extending to Southern China and enhancing the heavy rainfall locally. Especially in 2008 winter, several processes of a strong HV-WCP event followed by continuous weak ones are conducive to the low-temperature-precipitation disaster in Southern China.

Plain language summary

The wintertime Kuroshio sea surface temperature front in East China Sea is turned out to be relevant with the heavy precipitations in Southern China significantly. The strong HV-WCP events over Kuroshio front area, defined as the High-frequency Variability events of the sea surface Wind Coupled with Precipitation, determine more than half winter heavy precipitation events in

Southern China. Due to the significantly enhanced frontal intensity on the day before strong HV-WCP events, the initial precipitation appears in Middle-lower Yangtze River. After it moving to the Kuroshio front, the positive feedback between circulation, vapor transport and rainfall makes precipitation enhanced over Kuroshio front. Moreover, this positive feedback causes a large-scale stratus precipitation band extending to the Southern China, and strengthening the heavy rainfall there. The further results suggest that, on the interannual scale, the more C-events defined as a strong HV-WCP event followed by continuous weak ones over Kuroshio lead to more continuous low-temperature-precipitation winter days in Southern China, typically for the severe disaster period in 2008 early winter. Therefore, the HV-WCP events over Kuroshio front have potential prediction significance on persistent winter disasters in Southern China, which can be used to prevent social damages caused by the extreme synoptic events.

1 Introduction

Recently, the winter precipitation in Southern China has attracted extensive attention because it has an essential impact on agriculture, energy, water resources, transportation and communication in China, although winter precipitation in Southern China is typically weaker relative to spring or summer (Deng et al. 2012; Ren and Ren 2017; Xie et al. 2014b; Ye 2014; Zhou et al. 2011, 2017). The Southern China winter precipitation are affected by various atmospheric and oceanic factors, such as East Asia Winter Monsoon, the Madden-Julian Oscillation (MJO), El Niño-Southern Oscillation (ENSO) and the regional atmospheric circulations (Compo et al. 1999; Jia et al. 2011; Wang et al. 2000; Wu et al. 2003; Wu and Chan 1997; Yao et al. 2015; Zhou and Wu 2010; Zhou 2011). Besides, compared to other seasons, the winter atmosphere has some unique distinctions especially over East Asia. For instance, the prevailing land-to-sea circulations within marine atmospheric boundary layer (MABL) related to the winter monsoon and air-sea interaction (Cai et al. 2017) are the essential physical process in the prediction of the winter precipitation in Southern China.

For air-sea interaction process, the sea surface temperature (SST) over offshore sea and its obvious temperature gradient with land surface in winter play important role in modulating land precipitation. Recently, due to favorable development of high-resolution observations and numerical simulation, the importance of SST front in atmospheric circulation and rainfall variability has revealed gradually, which indicate the SST front can affect the free atmosphere and provide an anchor for rain bands by triggering deep cumulus convection along the warm current (Chen et al. 2019; Kuwano-Yoshida et al. 2010; Minobe et al. 2008; Tokinaga et al. 2006; Wen et al. 2019; Xu et al. 2011; Xu and Xu 2015). Especially in East China Sea (ECS), a distinct small-scale SST front due to the strong contrast between Kuroshio warm water and shelf cold water can lead to the significant heat, momentum and material exchange with the local atmosphere in the ECS, which has significant influences on the climate and weather in East Asia (Bryan et al. 2010; Bai et al. 2019; Chelton and Xie 2010; Small et al. 2008; Shimada and Kawamura 2008; Wang et al. 2019; Xu et al. 2011;

Xu and Xu 2015). Therefore, the role of Kuroshio SST front may also be significant on winter Southern China precipitation, however, it has not been carefully considered so far.

By investigating Kuroshio SST front impacts on the precipitation over surrounding area, Gan et al. (2019) indicated the precipitation significantly increase over the Yangtze River delta to Kyushu with Kuroshio shifts offshore in summertime, but its effects on winter precipitation are not clear. Using the high-resolution Weather Research and Forecasting (WRF) model, Xu et al. (2018) found the possible effects of Kuroshio SST front on Southeastern China winter rainfall. They showed the simulated heavy rainfall over Southeastern China will increase significantly when SST frontal intensity weakened. However, the results are based on numerical simulations, which have much uncertainty for different parameterization schemes and different resolutions, etc. Bai et al. (2020) found the special events over Kuroshio SST front in winter, which is defined High-frequency Variability events of the sea surface Wind Coupled with Precipitation (HV-WCP) events. The HV-WCP events are obviously different the sea-land breeze, and have significant effects on local rainfall anomalies over ECS. Previous studies have indicated that the precipitation over Kuroshio SST front can generate wider climate effects by affecting local circulation. So, is there a relationship between HV-WCP events and precipitation in Southern China? What is the specific dynamical mechanism?

Furthermore, for Chinese focused extreme disaster events during wintertime, the winter precipitation in Southern China is one of the crucial factors. Therefore, much attention has been paid to the extreme synoptic events over Southern China in winter, which has heavy losses in many aspects of China, such as the agriculture, the transportation, the electric power and so on. Especially in early 2008, unusually severe meteorological disasters occurred in Southern China from middle of January to the first decade of February and have severe damages, including low temperature, heavy precipitation and freezing (Ding et al., 2008; Li et al., 2008; Wang et al., 2008; Zhou et al., 2011, 2017). For the extreme persistent low-temperature-rainy events in winter of 2008, previous studies have proved it may be resulted from multiple atmospheric and ocean system anomalies, including the global warming, the La Nina situation, the activity of the atmospheric quasi-stationary front, the northward transport of warm water vapor from the Bay of Bengal, a transverse trough from Lake Baikal to Lake Balkhash and the Ural blocking high (Ding et al., 2008; Li et al., 2008; Qian et al., 2008; Qian et al., 2014). However, the potential roles of the Kuroshio SST front in the East China Sea on the winter extreme synoptic events in Southern China are paid little attention in previous studies.

Therefore, for the winter precipitation in Southern China and Kuroshio SST front, is there some relationship between them, especially for the heavy precipitation? If any relationship, what is the specific physical process that connects them? What role does Kuroshio SST front play for the extreme persistent low-temperature-precipitation disasters in Southern China? This study is de-

signed to investigate the specific relationship between the winter precipitation in Southern China and East China Sea Kuroshio SST front and associated specific physical progress. The paper is presented as follows. Section 2 describes the data and methods in this study. Section 3 explores the Kuroshio SST front effects on the winter precipitation in Southern China. Finally, the conclusion and discussion are presented in section 4.

2 Data and Methods

The hourly Products of the fifth generation European Center for Medium-Range Weather Forecasts (ECMWF) Atmospheric Reanalysis (ERA5) during wintertime of 1979-2020, the Version 7 precipitation product of Tropical Rainfall Measuring Mission 3B42 (TRMM) during wintertime of 1998-2020 and the precipitation product of 756 stations in China during wintertime of 1979-2020 are used in this study to analyze the precipitation in Southern China and Kuroshio SST front.

The ERA5 is the latest climate reanalysis produced by ECMWF, providing hourly data on many atmospheric, land-surface and sea-state parameters together with estimates of uncertainty. ERA5 combines model data with observations from across the world into a globally complete and consistent dataset using the laws of physics. Using the 4D-Var data assimilation method in Cycle 41R2 of ECMWF's Integrated Forecast System (IFS), it takes account of the exact timing of the observations and model evolution within the assimilation window. This hourly output resolution is quite an improvement with respect to the last generation ECMWF's reanalysis product (ERA-interim), and provides a more detailed evolution of particular weather events (https://confluence.ecmwf.int//pages/viewpage.action?pageId=74764925). ERA5 hourly data are available in the Climate Data Store on regular latitude-longitude grids at 0.25° x 0.25° resolution, with atmospheric parameters on 37 pressure levels from 1979 to present.

The TRMM precipitation product are provided by the National Aeronautics and Space Administration of the United States (NASA) and the Japan Aerospace Exploration Agency of Japan (https://giovanni.gsfc.nasa.gov), to monitor the precipitation over tropical and subtropical. The satellite was equipped with, the Microwave Imager, Precipitation Radar, Visible Infrared Scanner, Lightning Imaging Sensor, and Cloud and Earth Radiant Energy System. The area was 38°S to 38°N, 180°W to 180°E before the orbit change in August 2001, and 50°S to 50°N, 180°W to 180°E after orbit changing. The study mainly uses 3B42V7 Precipitation products during the winter of 1998 to 2020 through the Precipitation Radar PR. The 8 output times per day of the TRMM precipitation are 00:00, 03:00, 06:00, 09:00, 12:00, 15:00, 18:00, 21:00 UTC, with 0.25° x 0.25° spatial resolution.

The precipitation product of 756 stations in China provided by China National Meteorological Information Center (http://data.cma.cn/data/detail/dataCode/A.0012.0001.html). This study uses daily precipitation data from 756 stations

in China during the winter of 1979 to 2019. Although this station data lack of maritime observation results, the station information in China region has a high precision, thus is used to further verify the precipitation results of ERA5 reanalysis data over Southern China, to improve the reliability of analysis results and credibility.

Furthermore, to analyze the Kuroshio SST front effects on winter heavy rainfall in Southern China quantitatively, a series of high-resolution simulations of SST forcing over ECS were conducted utilizing WRF 3.9.1 model in our study. The WRF model is one of the most advanced regional meteorological models (Carvalho et al., 2014; Skamarock et al. 2008), which is developed by NCEP (National Centers for Environmental Prediction), NCAR (National Center for Atmospheric Research) and other institutions. The detailed design of WRF simulation is depicted in *Section 3.2*.

The HV-WCP events are defined as the High-frequency Variability events of the near-surface Wind Coupled with Precipitation events over Kuroshio SST front during wintertime (Bai et al., 2020). From morning to night on the day with the peak variability, the HV-WCP events is characterized as the change of surface wind directions from southerly anomaly to northwest anomaly and increasing wind speed, coupled with decreasing precipitation. The HV-WCP events have proved associated with significant climate effects on the rainfall anomaly over surrounding areas of ECS. HV-WCP index, representing the intensity of the high-frequency atmospheric variability, is calculated as the half sum of normalized variance of wind speed and normalized variance of wind direction, every day. Besides, the heavy precipitation here is defined as the daily precipitation rates with each grid/station exceeds 75% of its percentile.

3 Results

3.1 The observed precipitation relationship between Southern China and Kuroshio SST front

When the strong HV-WCP events occur over the Kuroshio SST front, Bai et al (2020) indicated that strong HV-WCP events will not only affect the local precipitation over the Kuroshio SST front, but also affect the stratus precipitation over surrounding areas of ECS, especially in the middle and lower reaches of the Yangtze River and southern China. Then, in winter, what specific impact does the HV-WCP strong event have on the precipitation in South China, and what specific mechanism does it affect the precipitation in South China? To settle this problem, this study will analyze the further connection between Kuroshio SST front and Southern China associated with HV-WCP events.

Firstly, from the winter mean state of precipitation and heavy precipitation in different data, it is obvious that there are two key regions of winter climate precipitation in reanalysis data (ERA5), station data and satellite data (TRMM), one is Kuroshio SST front and its warm current over ECS, and the other is Southern China (Fig. 1). In addition, through the analysis of precipitation and local circulation, Bai et al (2020) suggested that the significant positive feedback

process between precipitation and local circulation existed when the HV-WCP strong event occurs, the precipitation will be gradually enhanced through this positive feedback process at this time. Therefore, we hypothesize the precipitation associated with HV-WCP events should be a relatively heavy precipitation. The different data results show that, for heavy precipitation, there are still two key regions including Kuroshio SST front and associated warm flanks and Southern China.

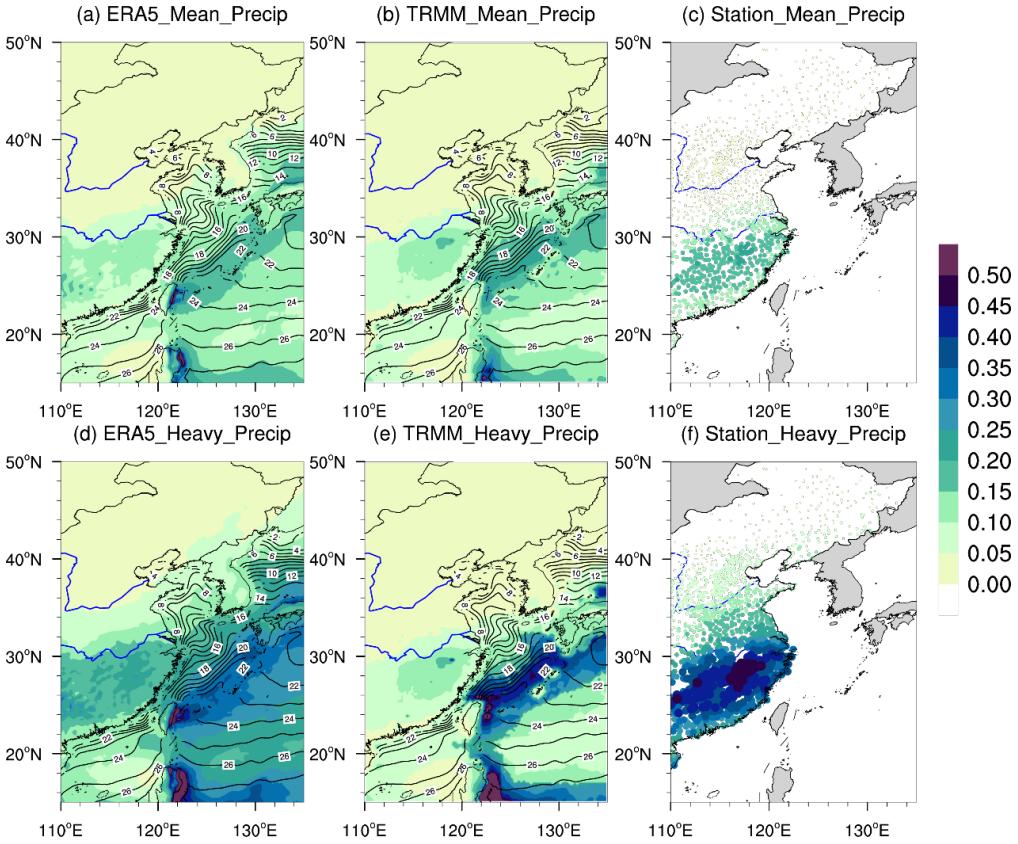

Figure 1. The distributions of winter mean precipitation (a, b, c) and heavy precipitation (d, e, f) (shadings, unit: mm/h). (a)(d), (b)(e) and (c)(f) are results of ERA5 data in winter from 1979 to 2019, TRMM data in winter from 1987 to 2019 and station data in winter from 1979 to 2019, respectively.

Besides, the heavy precipitation distributions here are apparently similar to the precipitation distribution obtained by regression when strong HV-WCP events occurred. The ERA5 precipitation of strong HV-WCP events (Fig. 2a) also shows two same significant regions at this time, including the Kuroshio region and its warm side over ECS, and the southern China. The correlation between strong HV-WCP events precipitation and winter mean heavy precipitation reaches 0.841, passed 99% confidence level. It indicates the significant

relationship between the strong HV-WCP events and the heavy precipitation in Southern China. We further calculated the regression result between HV-WCP index and heavy precipitation (Fig. 2d), which also indicated two same key regions, suggesting that when HV-WCP event is stronger, the associated heavy precipitation will be stronger over Kuroshio SST front and its warm side and Southern China. The HV-WCP strong events mainly affect the anomaly of heat flux through the thermal effects on both sides of Kuroshio, thus affecting the vertical structure of MABL, leading to the enhancement of local circulation and water vapor conditions, and further affecting precipitation (Bai et al., 2020). Therefore, the composite differences of sensible heat flux (SH), the differences between SST and 2m air temperature (SST-T2), latent heat flux (LH), planetary boundary layer height (PBLH) gradient and water vapor transport conditions between strong HV-WCP events and weak ones in ERA5 data were calculated (Fig. 2b, 2c, 2e, 2f), which show the upward SH and LH will weaken due to the weakening of the background winter monsoon when strong HV-WCP events occur over Kuroshio SST front, making the PBLH over Kuroshio SST front decrease on both cold and warm flanks but more on warm side, enhancing PBLH gradient over Kuroshio SST front. This process makes the water vapor transported from the warm side to the cold side cross the MABL top and enter free atmosphere to form significant water vapor convergence zone, resulting in heavy precipitation during strong HV-WCP events.

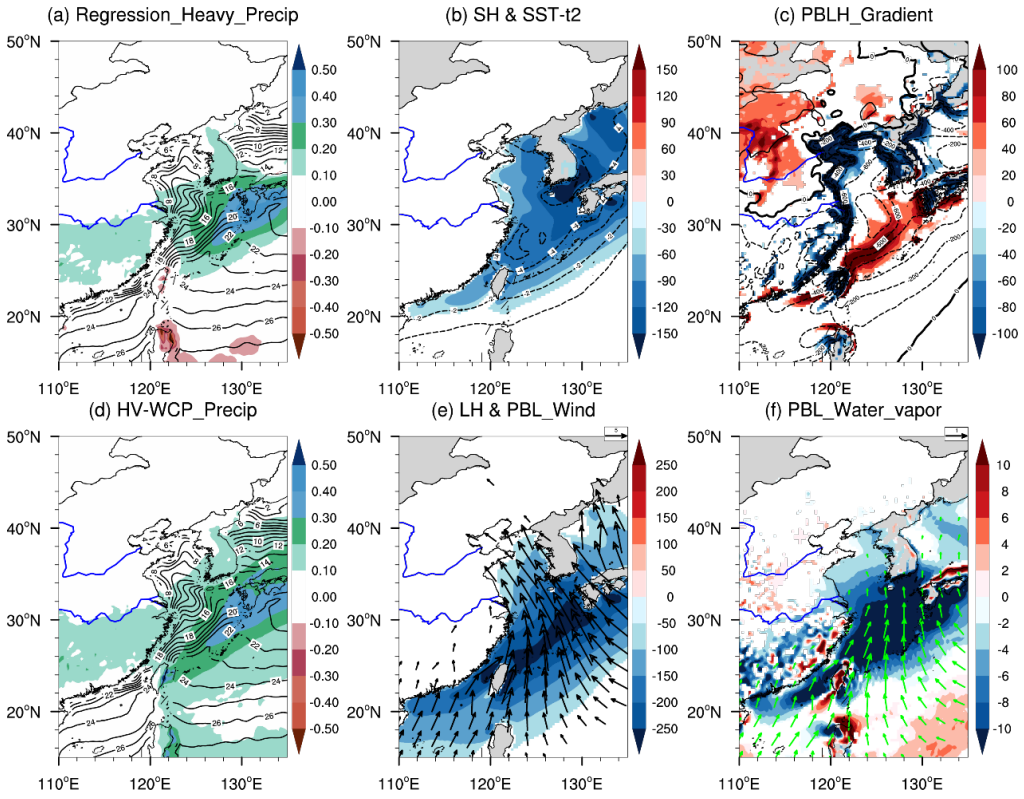

Figure 2. (a) is the distribution of SST (contours, units: ℃) and regression heavy precipitation (shadings, units: mm/h) with HV-WCP index in the ERA5 data from 1979 to 2019 wintertime; (b) is the SH (shadings, unit: W/m-2) difference and SST-T2 (contours, unit: ℃) between strong and weak HV-WCP events in ERA5 data from 1979 to 2019 wintertime; (c) is the difference of the PBLH gradient (shadings, units: m/0.25°) and the PBLH (contours , units: m) between strong and weak HV-WCP events in the ERA5 data from 1979 to 2019; (d) is the precipitation (shadings, units: mm/h) distribution of strong HV-WCP events in the ERA5 data from 1979 to 2019 wintertime; (e) is the SH (shadings, units: W/m-2) and the wind field within PBL (arrows, units: m/s) difference between strong and weak HV-WCP events in the ERA5 data from 1979 to 2019 wintertime; (f) is the water vapor flux (arrows, units: 10-7 g/(hPa*m*s)) and its divergence (shadings, units: 10-12 g/(hPa*m-2*s) difference within PBL between strong and weak HV-WCP events and of the winter ERA5 data from 1979 to 2019 wintertime. All shaded values exceed 95% confidence level.

The frontal process is a significant concept in the analysis of weather dynamics. The formation, strengthening, weakening and disappearance of atmospheric frontal plane will be accompanied by drastic changes in the weather near the cover. In winter, large-scale frontal system often appears in the Southern China, accompanied by cold wave, precipitation and other weather processes. Bai et al

(2020) have proved that, to sustain the strong HV-WCP events, the large-scale circulation needs to exhibit declines in the upstream monsoon and weakening vertical mixing in MABL. Therefore, in order to further analyze the whole evolution process of precipitation in southern China during the HV-WCP strong event and its relationship with large-scale cold and warm air activities, the study uses the frontogenesis function to calculate the evolution of frontogenesis intensity in the precipitation process. The formula for calculating frontogenesis strength is:

$$Fg23(\Theta) = -\frac{1}{2}\frac{1}{\nabla\Theta}(\nabla\Theta)^2 D_h - \frac{1}{2}\frac{1}{|\nabla\Theta|}\bullet\left\{\left[\left(\frac{\partial\Theta}{\partial x}\right)^2 - \left(\frac{\partial\Theta}{\partial y}\right)^2\right]A_f + 2\frac{\partial\Theta}{\partial x}\frac{\partial\Theta}{\partial y}B_f\right\} \quad (1)$$

where Θ is the specific humidity $D_h = \frac{\partial u}{\partial x} + \frac{\partial v}{\partial y}$; $A_f = \frac{\partial u}{\partial x} - \frac{\partial v}{\partial y}$; $B_f = \frac{\partial v}{\partial x} + \frac{\partial u}{\partial y}$.

As shown in Fig.3, Fig.S1 and Fig.S2, the results of frontogenesis intensity and precipitation evolution from the day before the strong event show that on the day before the HV-WCP strong event, due to the convergence of large-scale cold and warm air, the frontogenesis intensity increased significantly in the middle and lower reaches of the Yangtze River, so precipitation firstly appeared in the middle and lower reaches of the Yangtze River, and then the whole precipitation system moved southeast with the background winter monsoon, but the changes of precipitation intensity were not obvious. Until the precipitation moved into the Kuroshio SST front over ECS, due to the positive feedback system of local circulation and precipitation of SST front, the precipitation increased significantly after moving into the Kuroshio region, and reached its peak at 06:00LT in the morning. At this time, the maximum precipitation area was mainly located in the Kuroshio ocean front and its warm side, further extended Southern China and enhances the precipitation over there. When the whole coupling system continued to move southeast with the background winter monsoon and gradually moved out of the SST front, the precipitation gradually weakened and finally disappeared.

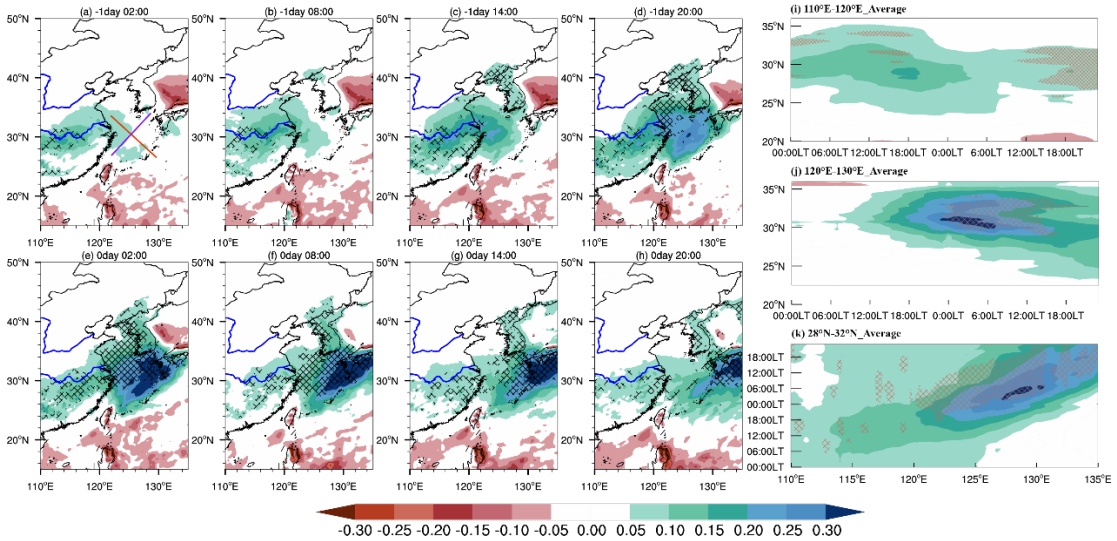

Figure 3. The precipitation variations (mm/h) of HV-WCP events over Kuroshio SST front during wintertime of 1979-2019 in ERA5 data at 02:00 LT (a, e), 08:00 LT (b, f), 14:00 LT (c, g), and 20:00 LT (d, h) respectively. (i), (j) and (k) are precipitation differences (shadings, unit: mm/h) and the frontal intensity differences (red lines shaded, exceeding the threshold 1^{-10}/s) over the land zonal profile (110°E-120°E), the ocean zonal profile (120°E-130°E) and the longitudinal profile (28°N-32°N), respectively. In (i) (j), X-axis is time and Y-axis is latitude. In (k), X-axis is longitude and Y-axis is time. All shaded values exceed 95% confidence level.

The MABL height and water vapor transport have obvious changes from two days before the strong HV-WCP events to the next day (Fig.4, Fig.S3-S6). Two days before the HV-WCP strong events, the MABL was lower on the cold side and higher on the warm side, but there was no significant difference between the cold and warm sides, and there was no significant difference between the boundary layer structure and the weak event, which means, the MABL gradient on the cold and warm sides changed little at this time, and its diurnal variation was also very weak. On the one day before the HV-WCP strong events, MBAL height gradient and the associated water vapor transport gradually enhanced. On the day of the HV-WCP strong event, due to the significant positive anomalies of MABL height gradient, the southeast water vapor anomaly will further make it easier for water vapor to enter the free atmosphere from the MABL across the top of MABL, thus bringing more water vapor convergence over the Kuroshio oceanic front and on the warm side. Moreover, the upward and westward water vapor transport and convergence will reach the maximum in the early morning of the day (around 06: 00LT), which also corresponds to the occurrence time of precipitation peak. The water vapor flux gradually weakened, and the water vapor convergence area gradually moved to the warm side of the Kuroshio SST front. On the evening of that day, although the upward water

vapor transport was still quite strong, the water vapor transport and convergence from the warm side of the Kuroshio SST front almost disappeared, and the precipitation gradually moved out of the Kuroshio SST front. On the day after the HV-WCP strong event, the precipitation system completely moved out of the SST front area, and the boundary layer height gradient on both sides of the Kuroshio SST front area weakened, so did the water vapor transport and its convergence, and the vertical structure and water vapor conditions of the boundary layer gradually returned to the state before the HV-WCP strong event.

Significantly, on the day of the HV-WCP strong event, although the boundary layer height gradient on both sides of the Kuroshio ocean front increased significantly, the daily variation of boundary layer height was very weak. However, at this time, the water vapor transport and convergence over the Kuroshio ocean front have a significant diurnal variation, and the water vapor conditions became significantly weaker from the early morning, which indicated that the diurnal variation of water vapor condition was not determined by the diurnal variation of vertical structure of boundary layer. Significantly enhanced MABL gradients on the cold and warm sides of the Kuroshio ocean front will cause a large amount of water vapor to be transported across the boundary layer top to the free atmosphere above the boundary layer, but it does not provide the conditions for producing significant diurnal variation of water vapor transport and convergence. The center of positive vorticity anomaly and the center of vertical upward movement moved from the cold side of Kuroshio to the southeast, all the way to the warm side of Kuroshio ocean front, and finally moved out of the ocean front. Vorticity anomaly and upward vertical movement can cause water vapor transport from the cold side to the warm side in the Kuroshio ocean front. The daily variation of local circulation is the main reason for determining the daily variation of water vapor conditions, while water vapor transport and convergence are the main reasons for precipitation. When precipitation occurs in the Kuroshio ocean front, the enhancement of low-level positive vorticity anomaly and upward movement caused by latent heat release from precipitation will further strengthen water vapor conditions, thus enhancing precipitation again.

The daily variation of local circulation is the main reason for determining the daily variation of water vapor conditions, while water vapor transport and convergence are the main reasons for precipitation. There is a significant positive feedback process between local circulation and precipitation, and precipitation is the key factor to stimulate the whole positive feedback. When precipitation moves into Kuroshio SST front, the enhancement of low-level positive vorticity anomaly and upward movement caused by the release of latent heat brought by precipitation will strengthen the water vapor condition, which will further enhance precipitation. When precipitation moves out of the SST front, the overall strength of the positive feedback system will weaken, and finally the anomalies of precipitation and local circulation will gradually weaken to the state before strong events.

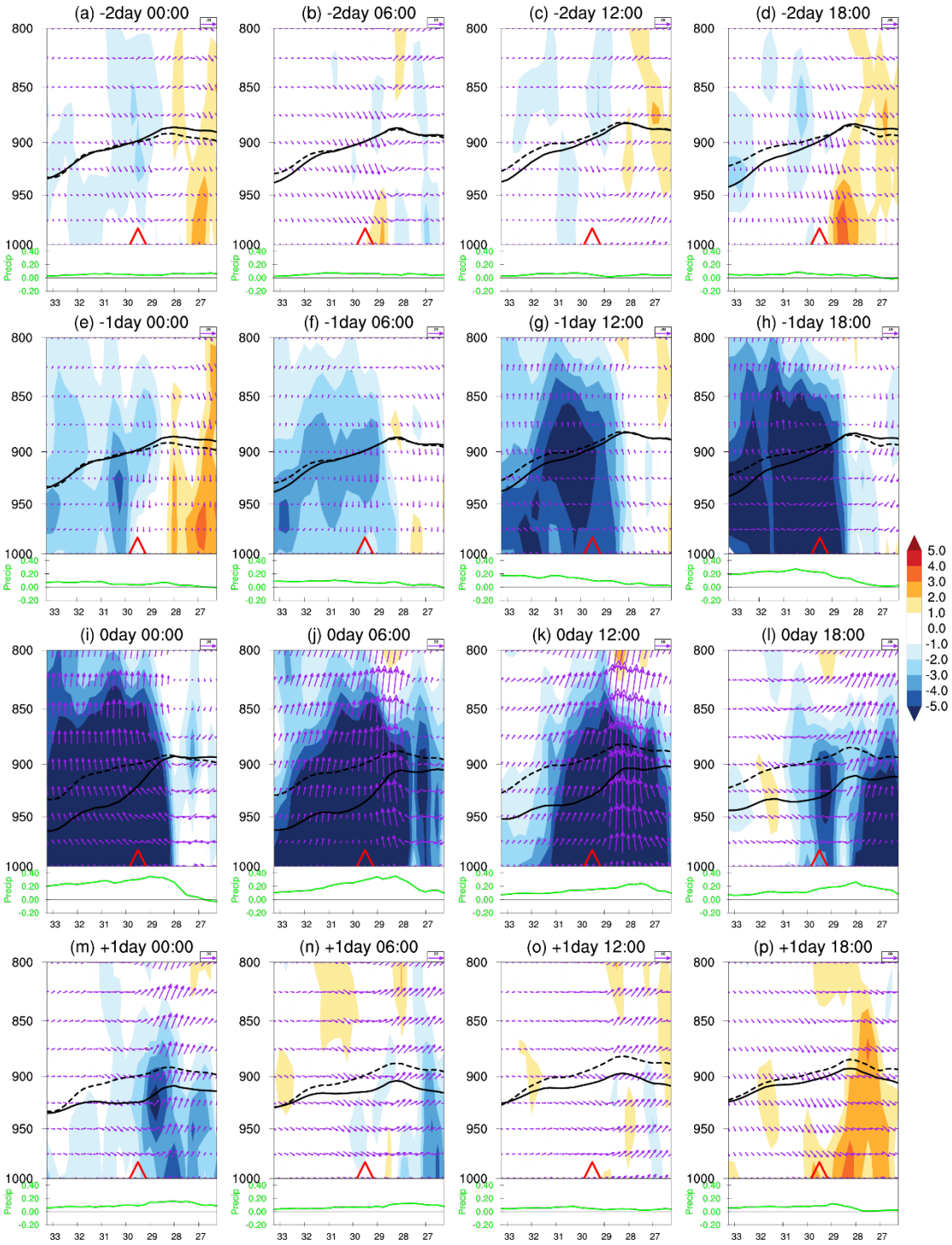
(a) -2day 00:00
(b) -2day 06:00
(c) -2day 12:00
(d) -2day 18:00
(e) -1day 00:00
(f) -1day 06:00
(g) -1day 12:00
(h) -1day 18:00
(i) 0day 00:00
(j) 0day 06:00
(k) 0day 12:00
(l) 0day 18:00
(m) +1day 00:00
(n) +1day 06:00
(o) +1day 12:00
(p) +1day 18:00
800
850
900
950
1000
Precip
0.40
0.20
0.00
-0.20
33 32 31 30 29 28 27
5.0
4.0
3.0
2.0
1.0
0.0
-1.0
-2.0
-3.0
-4.0
-5.0

Figure 4. The vertical cross sections of the water vapor transport (vectors; units: 10^{-7} g/(hPa*m*s)) and the divergence of the water vapor transport (shadings; units: 10^{-12} g/(hPa*m^{-2}*s)) against over Kuroshio SST front during the winters of 1979-2019 in ERA5 data at 02:00 LT, 08:00 LT, 14:00 LT, and 20:00 LT respectively. The green lines on the bottom panels represents the associated precipitation anomalies (units: mm/h). (a) (b) (c) (d), (e) (f) (g) (h), (i) (j) (k) (l) and (m) (n) (o) (p) are the lead 2 days, 1 day, 0 day and -1 day respectively. All shaded values exceed 95% confidence level.

3.2 The WRF simulation results of Kuroshio SST front contributions

Based on observation results, we cannot give a quantitative answer about the Kuroshio contributes to the heavy precipitation in Southern China. Therefore, based on WRF 3.9.1 model, which is widely recognized for studies of the medium and small-scale air-sea interaction (Song et al. 2009; Oneill et al., 2010; Xu et al., 2011; Xie et al., 2014a; Xu & Xu, 2015; Kilpatrick et al., 2016; Bai et al., 2019), we designed two high-resolution simulations of the SST forcing over the ECS to investigate Kuroshio SST front effects on winter heavy precipitation events in Southern China. One is the control (CTL) run experiment forced by the ERA5 2008 wintertime SST and the other is the smoothed SST (SmSST) run experiment in which the SST field is heavily smoothed by applying a two-dimensional 9-point averaging 100 times to decrease the SST gradient and remove the associated Kuroshio SST front (Fig. 5). To increase the signal-to-noise ratio, for CTL run experiment and SmSST run experiment, 10 ensemble members are run with different initial conditions, and their ensemble means are calculated, which indicate the atmospheric responses. The ensemble mean results of the SmSST run are regarded as the atmospheric response without the influence of the Kuroshio SST front. Therefore, the difference between the CTL run and SmSST run can be considered as the contribution of the Kuroshio SST front.

The model domain is 20.0–40.0° N, 110.0–130.0° E, with a relatively high horizontal resolution of 15 km and the 37 sigma levels in the vertical. The high-resolution ERA5 data are used as the lateral boundary conditions and initial field for the WRF simulation. The model output data is available at 1-hr intervals. The simulations are integrated during the wintertime of 2007–2008 (from the December 1st, 2007 to February 28th, 2008), when the significant low-temperature-precipitation disasters occurred in Southern China. The vital physical parameterization schemes used in the model include the Thompson microphysics scheme (Thompson et al. 2004), the Betts–Miller–Janjic scheme for cumulus parameterization (Janjić 1994, 2000), and the YSU atmospheric boundary layer parameterization scheme for the boundary layer (Hong et al. 2006).

Fig. 6 shows the HV-WCP index distributions in CTL and SmSST experiments and their differences. It is obvious that compared to CTL experiment, the HV-WCP index are reduced about 50% over ECS in SmSST experiment, which suggests the Kuroshio SST front have significant impacts on intensity of HV-WCP events. From the analysis of Section 3.1, the Kuroshio SST front

induced MABL prominent gradients over the cold and warm flanks caused abundant water vapor to be transported across the boundary layer top to the free atmosphere above the boundary layer and to form significant water vapor convergence zone, resulting in heavy precipitation during strong HV-WCP events. Thus, the decreasing of HV-WCP index in SmSST experiment may be due to the MABL structure differences between CTL and SmSST experiment, which have significant effects on water vapor transportation and consequent precipitation.

Therefore, we further analyzed the diurnal cycle of total precipitation and PBLH differences between CTL and SmSST experiments (Fig. 7). The simulation results indicated that, compared to CTL experiment, the PBLHs have remarkable reduction and decrease more over warm flank (more than 500m) in SmSST experiment, which cause PBLH gradient decreased significantly in SmSST experiment. Especially at 00:00LT and 06:00LT, the PBLHs over warm flank are almost consistent with cold flank and the PBUH gradients are close to zero. It suggests that, with the reduction SST gradients in SmSST experiment, the PBLH structure will have obvious responses and induce significant decreasing of HV-WCP events intensity. Consequently, the precipitation will be reduced dramatically over, Kuroshio SST front in SmSST experiment. From 00:00LT to 18:00LT on strong HV-WCP events day, the precipitation reduction center moved eastward from Southern China coast to warm flank of Kuroshio SST front, which is corresponding to the observed rainband diurnal variations. Therefore, the simulation results proved that the Kuroshio SST front plays an important role on precipitation in Southern China and the MABL height gradient over the Kuroshio front is a critical factor in this process where the initial rainfall caused by the atmospheric frontal disturbances.

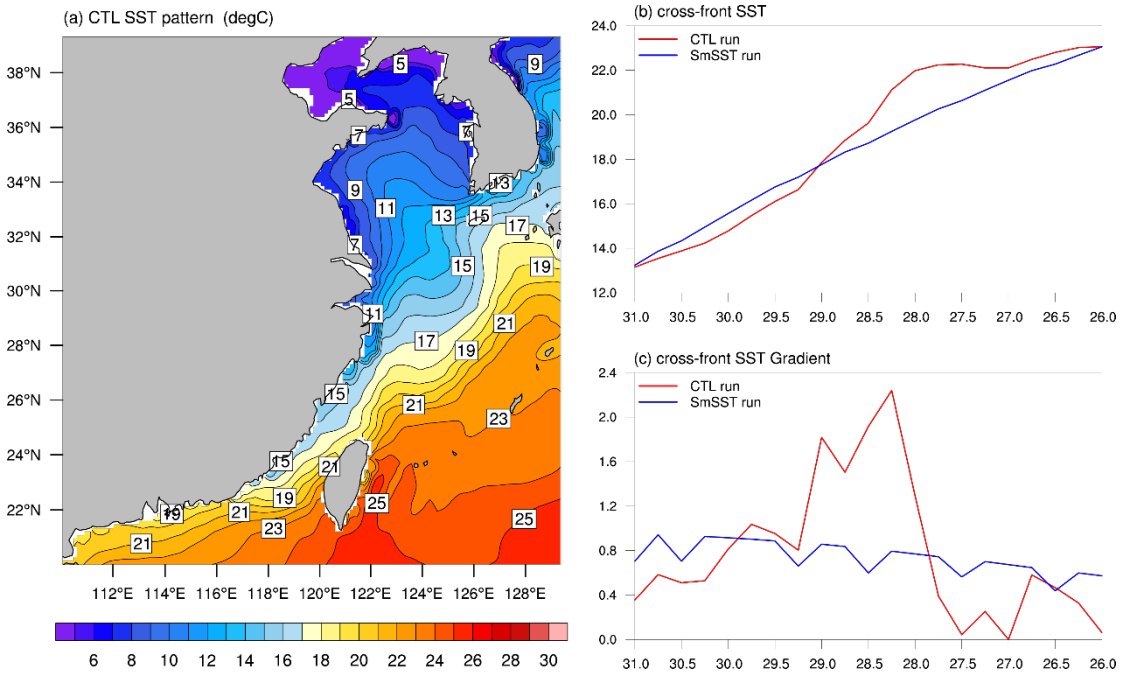

Figure 5. (a) The map of SST (colored; ℃) of WRF CTL experiment. (b) The mean SST (℃) perpendicular to the Kuroshio SST front and (c) the SST gradient (℃/100km) perpendicular to the Kuroshio SST front of the CTL and SmSST experiments. The red lines represent the CTL experiment results, the blue lines represent the SmSST experiments respectively and X-coordinate represents the latitude.

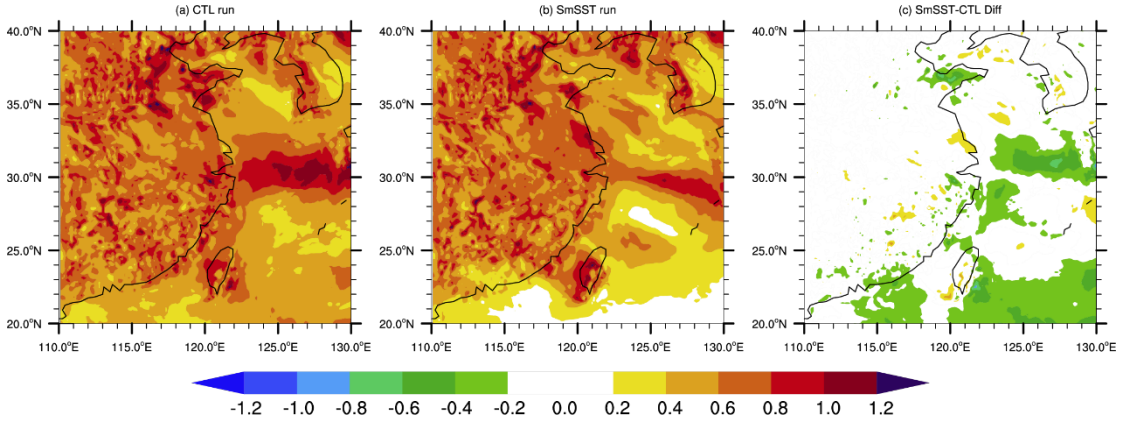

Figure 6. The HV-WCP index distributions of (a) the WRF CTL experiment, (b) the WRF SmSST experiment and (c) differences between SmSST experiment and CTL experiment.

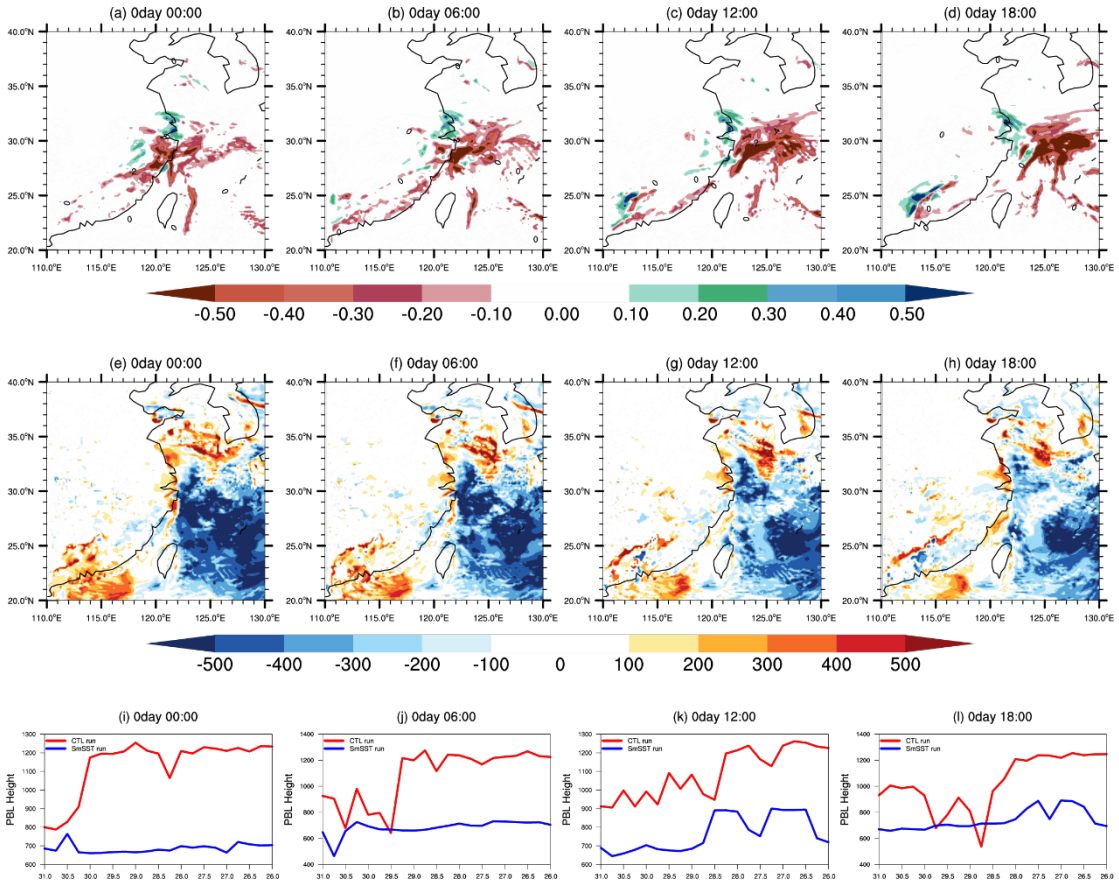

Figure 7. (a), (b), (c), (d) are total precipitation (colored; mm/h) differences between SmSST experiment and CTL experiment of strong HV-WCP events. (e), (f), (g), (h) are PBLH (colored; m) differences between SmSST experiment and CTL experiment of strong HV-WCP events. (i), (j), (k), (l) are PBLH (colored; m) perpendicular to the Kuroshio SST front of CTL experiment (red lines) and SmSST experiment (blue lines) of strong HV-WCP events.

3.3 The strong-weak combined HV-WCP events effects on Southern China during 2008 wintertime

The above analysis shows that the strong HV-WCP event will not only affect the precipitation over the Kuroshio SST front, but also further affect the precipitation in Southern China through the positive feedback process of precipitation system and local circulation. However, in the actual weather process, how are HV-WCP strong events and weak events distributed, and what different influences on precipitation of different intensity HV-WCP combined? The study counts the distribution of the number of strong and weak events in HV-WCP every year. The results show that the relationship between the number of strong and weak events in HV-WCP is not consistent. In some years, the number of

strong events is more than that of weak events, in some years, the number of strong events is less than that of weak events, and in some years, they are the same, and both have significant interannual variations. In early 2008, the severe low temperature, heavy snowfall and freezing events happened in middle-lower reaches of the Yangtze River valley and the areas to the south of the Yangtze River, have the severe damages in Southern China. Previous studies have proved that the anomalies of La Nina, subtropical high, south branch trough and polar vortex are the causes of this continuous freezing rain and snow event (Ding et al., 2008; Li et al., 2008; Qian et al., 2008; Qian et al., 2014). Then, during early 2008 wintertime, what is the relationship between the precipitation and abnormal circulation caused by HV-WCP event and this persistent low-temperature precipitation events?

Thus, the relationship between the HV-WCP event index of Kuroshio SST front and the abnormal evolution of temperature and precipitation were investigated over South China and ECS during the period from January 10, 2008 to February 11, 2008, when meteorological disaster events were most significant. The results (Fig. 8) show that there are three significant low-temperature-precipitation disasters in Southern China, and the three processes are characterized with rainy or snowy days firstly, then continuous low-temperature process, and finally lead to continuous low-temperature-precipitation disaster. When the persistent low-temperature-precipitation disaster occurs, the strong HV-WCP event will be followed by the weak HV-WCP events for several consecutive days, which suggest a persistent low-temperature-precipitation disaster in Southern China corresponds to a process in which a strong HV-WCP event occurs and then follows the weak ones for more than three days. The strong HV-WCP events will cause significant precipitation process, while the weak events correspond to significant temperature-fall process. Therefore, the study then defined the special combined HV-WCP event (C-event) as a strong HV-WCP event followed by continuous (more than 3 days) weak ones.

C-events have significant impacts on low-temperature-precipitation disaster in Southern China. When the winter background monsoon weakens and strong HV-WCP events occur, the warm and humid air from the warm side to the cold side will easily enter the free atmosphere from the MABL due to the existence of positive feedback over Kuroshio SST front, causing precipitation enhanced over Kuroshio SST front and Southern China. After that, with the winter monsoon and associated cold air activity will increasing, the weak HV-WCP events occur and it will invade Southern China for several days, causing the temperature to continue to drop significantly in the next few days. The cold and warm air met continuously in Southern China with the close intensity and lasted for a long time, which eventually led to a significant continuous low-temperature-precipitation disaster in Southern China.

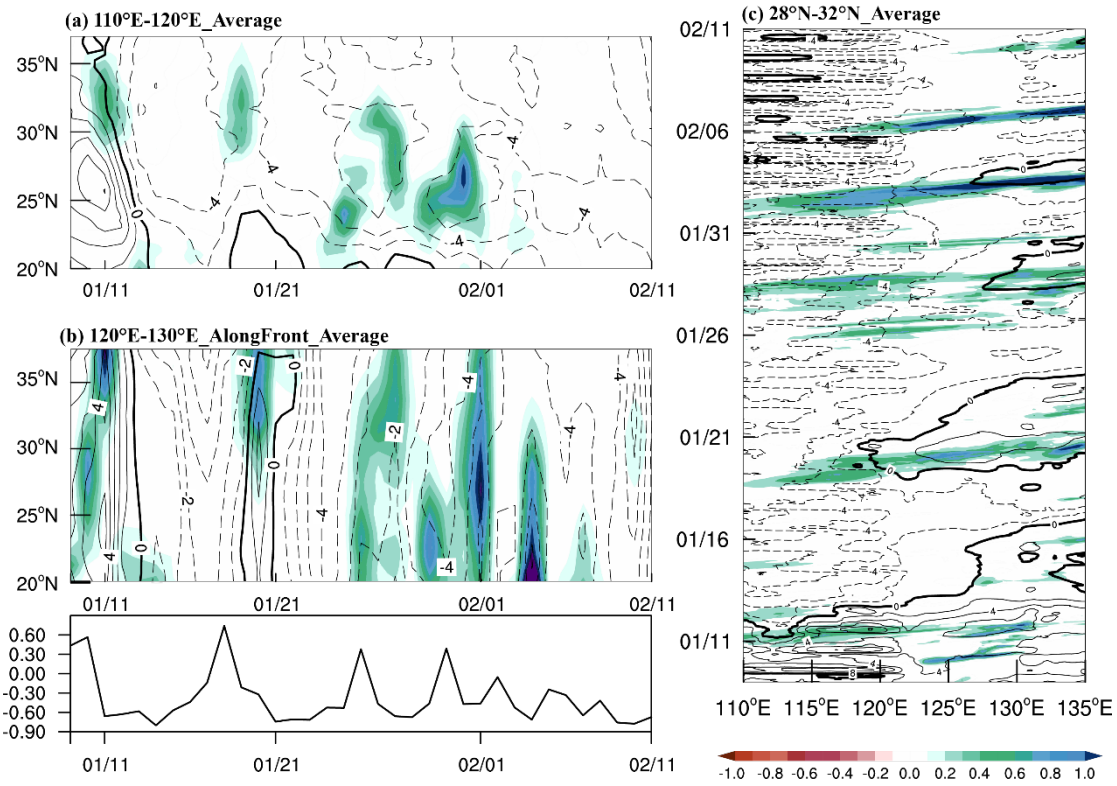

Figure 8. Precipitation anomalies from 2008/01/10 to 2008/02/11 in ERA5 data (shadings, units: mm/h) and temperature anomalies (contours, units: ℃) over profile (110°E-120°E), (120°E-130°E), and (28°N-32°N), respectively. In (a) and (b), X-axis is time and Y-axis is latitude. The bottom panels in (a) and (b) is the HV-WCP index in corresponding time period, where X-axis is time and Y-axis is intensity. In (c), X-axis is longitude and Y-axis is time. All shaded values exceed 95% confidence level.

For low-temperature-precipitation disaster in Southern China in the 2008 winter, previous studies have emphasized the integrated vapor transport (IVT) from the Indian Ocean to Southern China (Ding et al. 2008; Li et al. 2008; Qian et al. 2014). IVT is calculated as following formula:

$$IVT = \frac{1}{g}\int_{p_t}^{p_s} q\mathbf{V}\mathrm{dp} \tag{2}$$

where g represents the gravitational acceleration (m s^{-2}), q is the specific humidity (kg kg^{-1}), p_s is set to 1000 hPa, p_t is set to 300 hPa, p is the pressure (hPa), and $\mathbf{V}$ is the horizontal wind vector (m s^{-1}). They pointed out that water vapor transport from the Indian Ocean was the main cause of the anomaly in 2008 of the significant winter low-temperature-precipitation disasters in South

China. However, the calculation of IVT (formula 2) involves the integral of the whole layer as well as two physical quantities of water vapor content and wind speed. The lower atmosphere usually has more moisture than the upper atmosphere, but the vertical distribution of wind speed is the opposite. Therefore, it is necessary to further divide the previous full-layer IVT calculation into water vapor transport in the atmospheric boundary layer and water vapor transport in the middle-high atmosphere to better reflect the influence of water vapor content and source. In order to calculate the contribution of low-level water vapor and middle-high level water vapor, this study calculated the water vapor integral of the whole layer and boundary layer, and divided by the integral height to calculate the water vapor transport per unit height.

From the previous analysis in this study, when the HV-WCP strong events occur, there will be a significant transport of warm and moist air flows from the western Pacific Ocean, especially from the Kuroshio warm side in the ECS to the Southern China. Therefore, we further analyzed the water vapor transport during a severe low-temperature-precipitation disaster in early winter of 2008. In order to calculate the contribution of low-level water vapor and middle-high level water vapor, this study further calculated the water vapor integral of the whole layer and boundary layer, and divided by the integral height to calculate the water vapor transport per unit height. In addition, previous studies have primarily emphasized IVT over time averaging throughout the winter of 2008. However, the real winter precipitation in South China is time discontinuous, and the contribution of water vapor transport in non-precipitation days and continuous precipitation days to precipitation in South China should be different. Therefore, in this paper, the atmospheric water vapor transport in the boundary layer and the middle-high layer are further divided into winter mean of 2008 (Fig. 9b, 9f), the months of low-temperature-precipitation disasters occurring (Fig. 9c, 9g), the days of low-temperature-precipitation disasters (Fig. 9d, 9h).

The results show that (Fig. 9), for the climate state, the whole layer of water vapor is obviously transported from the Indian Ocean to the Southern China, which produced convergent water vapor transport, while the lower layer of water vapor transport from the Indian Ocean is not obvious, but mainly the cold air from the high latitude accompanied by the winter monsoon. For the whole winter of 2008, there is significant warm and humid air from the Indian Ocean in the whole layer of water vapor transport, but there is no significant water vapor convergence area in southern China, and there is little convergence in the lower layer of water vapor at this time. Compared to winter-mean moisture sources from Indian Ocean, significant moistures transport from warm flank of Kuroshio SST front to Southern China within MABL, then induce moisture convergence during the disaster period, especially on the day with prominent precipitation anomalies.

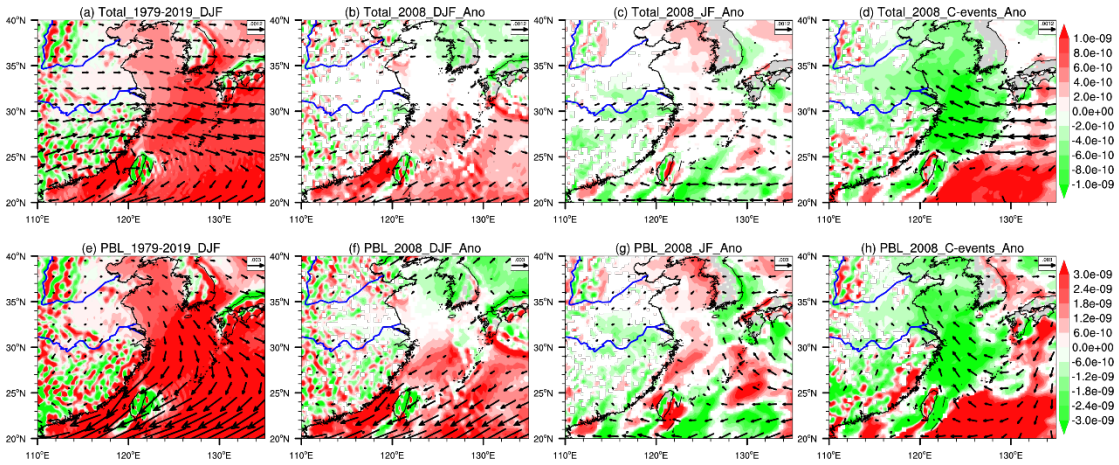

Figure 9. (a) is the water vapor flux per hPa (arrows, unit: g/(hPa*m*s)) and its divergence (colored, units: g/(hPa*m-2*s)) of the whole layer of climate state in the winter ERA5 data from 1979 to 2019; (b) is the anomaly of water vapor flux per hPa in the winter of 2008 (arrows, units: g/(hPa*m*s)) and its divergence anomaly (colored, unit: g/(hPa*m-2*s)); (c) The water vapor flux anomaly per hPa (arrows, units: g/(hPa*m*s)) and its divergence anomaly per hPa (colored, units: g/(hPa*m-2*s)) from January to February 2008; (d) is the anomaly of water vapor flux per hPa (arrows, units: g/(hPa*m*s)) and its divergence anomaly (colored, units: g/(hPa*m-2*s)) in C-Events from January to February 2008. (e, f, g, h) is the same as the variables in (a, b, c, d) but is the result of each hPa in the boundary layer. All shaded values exceed 95% confidence level.

Several synoptic processes during the low-temperature-precipitation disaster period closely related with HV-WCP events over Kuroshio front, which strong HV-WCP events correspond to rainy or snowy days in Southern China, while following weak events correspond to the temperature-fall days. It is obvious that warm and humid water vapor transported from the warm side to the cold side of the Kuroshio SST front both in the middle and upper layers and in the boundary layer at this time, and there will be significant water vapor convergence in the Kuroshio cold sides and in Southern China. Therefore, for the low-temperature-precipitation disasters in southern China in the winter of 2008, except the warm and humid air from Indian Ocean to southern China, from the Kuroshio warm side in the western Pacific Ocean, especially in the ECS, is more important for C-events, which are key events associated with low-temperature-precipitation disasters. In order to prove the importance of C-events defined by HV-WCP index, this study calculated the interannual correlation between the C-event numbers over Kuroshio front and days of persistent low-temperature-precipitation disasters in Southern China from 1979 to 2019 wintertime. The significant positive correlation (Fig. 10) indicates that C-events may be regarded as an early target for the winter low-temperature-precipitation disasters

in Southern China.

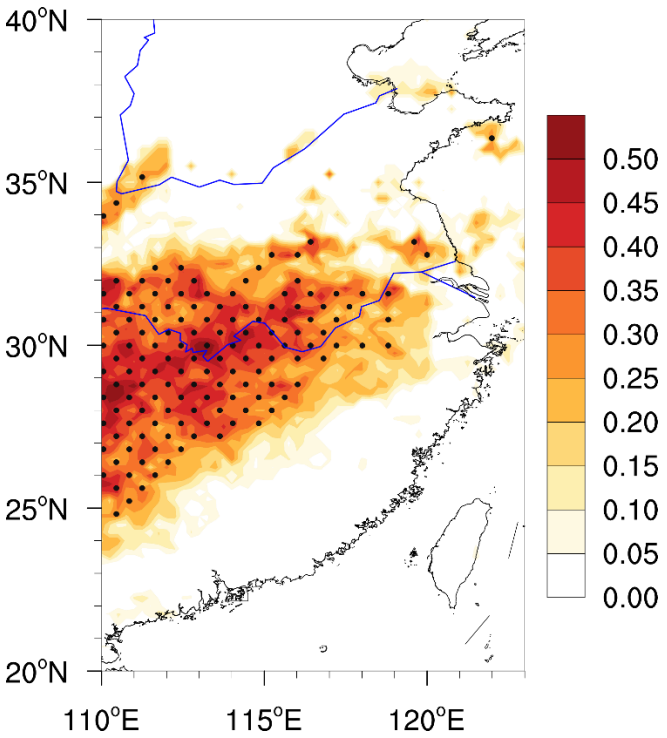

Figure 10. Interannual correlation coefficient (colored) of regional average days of low-temperature precipitation in Southern China and regional average number of C-events in winter ERA5 data from 1979 to 2019. Dotted values exceed 95% confidence level.

4 Conclusions and Discussions

The study investigated the special effects of high-frequency wind-coupled-precipitation events over Kuroshio SST front on winter heavy precipitation in Southern China, especially for the persistent low-temperature-precipitation events. The results indicated that when strong High-frequency Variability events of the sea surface Wind Coupled with Precipitation (HV-WCP) events occur over East China Sea Kuroshio front, it will not only influence the local precipitation, also affect the rainfall in Southern China due to the positive feedback between the precipitation and atmospheric circulation. Furthermore, the increase of the Kuroshio SST front MABL height gradient has played a very critical role in the process where the initial precipitation is the key inspiring factor.

Compared to the summer results (Liu et al. 2020), caused by the significantly enhanced frontal intensity with the large-scale warm and cold air converges in winter, the initial precipitation appears in the middle and lower reaches of

the Yangtze River. When it moving to Kuroshio SST front area because of the winter monsoon, the precipitation generates a low-level cyclone and southeasterly wind anomalies. With the pronounced marine atmospheric boundary layer (MABL) height gradient over Kuroshio SST front during strong HV-WCP events, the southeasterly wind anomalies transport plentiful moisture from PBL to the free atmosphere, generate significant water vapor convergence and induce precipitation. Then the precipitation leads to positive vorticity anomalies within MABL and enhanced upward airflow, which further strengthens the water vapor convergence and local precipitation. Therefore, this positive feedback process causes the large-scale stratus precipitation band extended to Southern China and determines its heavy-rainy days.

For the typical low-temperature-precipitation disasters in Southern China, the strong HV-WCP events will cause significant precipitation process, while the weak HV-WCP events correspond to a significant cooling process. When winter background wind weakened, due to the existence of positive feedback between precipitation and local circulation over the Kuroshio SST front, the warm and humid air from the warm side to the cold side will easily enter the free atmosphere from the boundary layer, causing precipitation enhanced over Kuroshio SST front and Southern China. At the same time, because the intensity of cold and warm air is close to each other, they continue to converge in the southern region of China and last for several days, so it has a significant impact on the persistent low-temperature-precipitation disasters in southern China.

Recently, with global warming, the extreme synoptic events in Southern China in winter occur frequently and attract much attentions. Typically, in 2008 early winter, a severe low-temperature-precipitation disaster happened in Southern China. Several synoptic processes of a heavy rainy or snowy day with followed persistent low-temperature days in Southern China were observed during this disaster period, which had close relationship with C-events (the special combined event with a strong HV-WCP event followed by continuous weak ones) over Kuroshio SST front. Different from previous studies (Ding et al. 2008; Li et al. 2008; Qian et al. 2014), we further found that, compared to winter-mean integrated vapor transport (IVT) from Indian Ocean to Southern China, the obvious water vapor within MABL transported northwestly from the Kuroshio warm side to Southern China caused during strong HV-WCP events. The subsequent low-temperature events related with continuous weak HV-WCP events. It implies the numbers of winter C-event over Kuroshio SST front have potential prediction significance on persistent low-temperature-precipitation disasters in Southern China, which can be used to reduce social damages of extreme synoptic events and still need further investigation.

Acknowledgments

Haibo Hu and Haokun Bai contribute equally as first authors. This work was supported by the National Key Program for Developing Basic Science (2022YFE0106600), the National Natural Science Foundation of China (grants 42175060, 41330420, 41621005, 41675064, 41675067, and 41875086), the Jiangsu

Province Science Foundation (Grant No. BK20201259). The authors are thankful for the support of the Jiangsu Provincial Innovation Center for Climate Change and Fundamental Research Funds for the Central University.

Open Research

The ERA5 hourly data are available through ECWMF's Climate Data Store at https://cds.climate.copernicus.eu/cdsapp#!/dataset/reanalysis-era5-single-levels?tab=form and https://cds.climate.copernicus.eu/cdsapp#!/dataset/reanalysis-era5-pressure-levels?tab=form. TRMM 3B42V7 Precipitation products are available at https://disc.gsfc.nasa.gov/datasets/TRMM_3B42_7/summary and the 756 stations precipitation product in China is available at http://data.cma.cn/data/detail/dataCode/A.0012.0001.html.

References

Bai, H., Hu, H., Yang, X.-Q., Ren, X., Xu, H., Liu, G. (2019). Modeled MABL responses to the winter Kuroshio SST front in the East China Sea and Yellow Sea. *Journal of Geophysical Research-Atmospheres*, *124*(12): 6069-6092. https://doi.org/10.1029/2018JD029570

Bai, H., Hu, H., Perrie, W., & Zhang, N. (2020). On the characteristics and climate effects of HV-WCP events over the Kuroshio SST front during wintertime. *Climate Dynamics, 55*(7), 2123-2148. https://doi.org/10.1007/s00382-020-05373-5

Bryan, F. O., Tomas, R., Dennis, J. M., Chelton, D. B., Loeb, N. G., & McClean, J. L. (2010). Frontal Scale Air-Sea Interaction in High-Resolution Coupled Climate Models. *Journal of Climate, 23*(23), 6277-6291. https://doi.org/10.1175/2010JCLI3665.1

Cai, R., Tan, H., & Kontoyiannis, H. (2017). Robust Surface Warming in Offshore China Seas and Its Relationship to the East Asian Monsoon Wind Field and Ocean Forcing on Interdecadal Time Scales. *Journal of Climate, 30*(22), 8987-9005. https://doi.org/10.1175/JCLI-D-16-0016.1

Carvalho, D., Rocha, A., Gómez-Gesteira, M., & Santos, C. S. (2014). Sensitivity of the WRF model wind simulation and wind energy production estimates to planetary boundary layer parameterizations for onshore and offshore areas in the Iberian Peninsula. *Applied Energy*, 135(2), 234–246. https://doi.org/10.1016/j.apenergy.2014.08.082

Chelton, D. B., & Xie, S. P. J. O. (2010). Coupled Ocean-Atmosphere Interaction at Oceanic Mesoscales. *23*(4).

Chen, Q., Hu, H., Ren, X., Yang, X.-Q. (2019). Numerical Simulation of Midlatitude Upper-Level Zonal Wind Response to the Change of North Pacific Subtropical Front Strength. *Journal of Geophysical Research-Atmospheres, 124*(9): 4891-4912. https://doi.org/10.1029/2018JD029589

Compo, G. P., Kiladis, G. N., & Webster, P. J. (1999). The horizontal and

vertical structure of east Asian winter monsoon pressure surges. *125*(553), 29-54. https://doi.org/10.1002/qj.49712555304

Deng, D., Gao, S., Du, X., & Wu, W. (2012). A diagnostic study of freezing rain over Guizhou, China, in January 2011. *138*(666), 1233-1244. https://doi.org/10.1002/qj.981

Ding, Y., Wang, Z., Song, Y., & Zhang, J. (2008). Causes of the unprecedented freezing disaster in January 2008 and its possible association with the global warming. *Acta Meteorologica Sinica, 66*(5):808-825. https://doi.org/10.3321/j.issn:0577-6619.2008.05.014

Gan, B., Kwon, Y.-O., Joyce, T. M., Chen, K., & Wu, L. (2019). Influence of the Kuroshio Interannual Variability on the Summertime Precipitation over the East China Sea and Adjacent Area. *Journal of Climate, 32*(8), 2185-2205. https://doi.org/10.1175/JCLI-D-18-0538.1

Hong, S-Y., Noh, Y., Dudhia, J. (2006). A new vertical diffusion package with an explicit treatment of entrainment processes. *Monthly Weather Review, 134,* 2318–2341. https://doi.org/10.1175/MWR3199.1

Janjić, Z.I. (1994). The step-mountain eta coordinate model: further developments of the convection, viscous sublayer, and turbulence closure schemes. *Monthly Weather Review, 122*, 927–945. https://doi.org/10.1175/1520-0493(1994)1222.0.CO;2

Janjić, Z.I. (2000). Comments on "Development and evaluation of a convection scheme for use in climate models". *Journal of Atmosphere Science, 57,* 3686–3686. https://doi.org/10.1175/1520-0469(2000)05760;3686:CODAEO62;2.0.CO;2

Jia, X., Chen, L., Ren, F., & Li, C. (2011). Impacts of the MJO on winter rainfall and circulation in China. *Advances in Atmospheric Sciences, 28*(3), 521-533. https://doi.org/10.1007/s00376-010-9118-z

Kilpatrick, T., Schneider, N., & Qiu, B. (2016). Atmospheric response to a midlatitude SST front: Alongfront winds. *Journal of Atmospheric Sciences,* 73(9), 3489–3509. https://doi.org/10.1175/JAS-D-15-0312.1

Kuwano-Yoshida, A., Minobe, S., & Xie, S.-P. (2010). Precipitation Response to the Gulf Stream in an Atmospheric GCM. *Journal of Climate, 23*(13), 3676-3698. https://doi.org/10.1175/2010JCLI3261.1

Liu, B., Yan, Y., Zhu, C., Ma, S., & Li, J. (2020). Record-breaking Meiyu rainfall around the Yangtze River in 2020 regulated by the subseasonal phase transition of the North Atlantic Oscillation. *Geophysical Research Letters*, 47, e2020GL090342. https://doi.org/10.1029/2020GL090342

Li, C.-Y., Yang, H., & Gu, W., (2008). Cause of Severe Weather with Cold Air, Freezing Rain and Snow over South China in January 2008. *Climatic and Environmental Research, 2008*(02), 113-122.

https://doi.org/10.3878/j.issn.1006-9585.2008.02.01

Minobe, S., Kuwano-Yoshida, A., Komori, N., Xie, S.-P., & Small, R. J. (2008). Influence of the Gulf Stream on the troposphere. *Nature, 452*(7184), 206-209. https://doi.org/10.1038/nature06690

O'Neill, L. W., Esbensen, S. K., Thum, N., Samelson, R. M., & Chelton, D. B. (2010). Dynamical analysis of the boundary layer and surface wind responses to mesoscale SST perturbations. *Journal of Climate*, 23(3), 559–581. https://doi.org/10.1175/2009JCLI2662.1

Qian, W. H., & Fu, J. L. Frontal genesis of moisture atmosphere during the early 2008 persistent freezing-rain event in southern China. (2009). *Science China Ser D-Earth Science, 39*(6), 387-398. https://doi.org/10.1007/s11430-009-0101-4

Qian, X., Miao, Q., Zhai, P., & Chen, Y. (2014). Cold–wet spells in mainland China during 1951–2011. *Natural Hazards, 74*(2), 931-946. https://doi.org/10.1007/s11069-014-1227-z

Ren, H.-L., & Ren, P. (2017). Impact of Madden–Julian Oscillation upon Winter Extreme Rainfall in Southern China: Observations and Predictability in CFSv2. *8*(10), 192. https://doi.org/10.3390/atmos8100192

Shimada, T., & Kawamura, H. (2008). Satellite evidence of wintertime atmospheric boundary layer responses to multiple SST fronts in the Japan Sea. *35*(23). https://doi.org/10.1029/2008GL035810

Skamarock, W. C., Klemp, J. B., Dudhia, J., Gill, D. O., Barker, D. M., Duda, M. G., et al. (2008). A description of the Advanced Research WRF Version 3. Rep. NCAR/TN–475+STR, Natl. Cent. for Atmos. Res., Boulder, Colo.

Small, R. J., deSzoeke, S. P., Xie, S. P., O'Neill, L., Seo, H., Song, Q., et al. (2008). Air–sea interaction over ocean fronts and eddies. *Dynamics of Atmospheres and Oceans, 45*(3), 274-319. https://doi.org/10.1016/j.dynatmoce.2008.01.001

Song, Q., Chelton, D. B., Esbensen, S. K., Thum, N., & Neill, L. W. O. (2009). Coupling between sea surface temperature and low-level winds in mesoscale numerical models. *Journal of Climate,* 22(1), 146–164. https://doi.org/10.1175/2008JCLI2488

Thompson, G., Rasmussen, R.M., Manning, K. (2004) Explicit forecasts of winter precipitation using an improved bulk microphysics scheme. Part I: description and sensitivity analysis. *Monthly Weather Review, 132,* 519–542. https://doi.org/10.1175/1520-0493(2004)132%3C0519:EFOWPU%3E2.0.CO;2

Tokinaga, H., Tanimoto, Y., Nonaka, M., Taguchi, B., Fukamachi, T., Xie, S.-P., . . . Yasuda, I. (2006). Atmospheric sounding over the winter Kuroshio Extension: Effect of surface stability on atmospheric boundary layer structure. *33*(4). https://doi.org/10.1029/2005GL025102

Wang, B., Wu, R., & Fu, X. (2000). Pacific-East Asian Teleconnection: How Does ENSO Affect East Asian Climate? *Journal of Climate, 13*(9), 1517-1536.

https://doi.org/10.1175/15200442(2000)013<1517:PEATHD>2.0.CO;2

Wang, L., Hu, H., & Yang, X. (2019). The atmospheric responses to the intensity variability of subtropical front in the wintertime North Pacific. *Climate Dynamics, 52*(9), 5623-5639. https://doi.org/10.1007/s00382-018-4468-9

Wang, Z., Zhang, Q., Chen, Y., Zhao, S., Zeng, H., Zhang, Y., & Liu, Q. (2008). Characters of Meteorological Disasters Caused by the Extreme Synoptic Process in Early 2008 over China. *Climate Change Research, 4*(2): 63-67. https://doi.org/10.3969/j.issn.1673-1719.2008.02.001

Wen, Z., Hu, H., Song, Z., Wang, Z. (2019). Different Influences of Mesoscale Oceanic Eddies on the North Pacific Subsurface Low Potential Vorticity Water Mass Between Winter and Summer, *Journal of Geophysical Research-Oceans, 125*(1): e2019JC015333. https://doi.org/10.1029/2019JC015333

Wu, M. C., & Chan, J. C. L. (1997). Upper-Level Features Associated with Winter Monsoon Surges over South China. *Monthly Weather Review, 125*(3), 317-340. https://doi.org/10.1175/15200493(1997)125<0317:ULFAWW>2.0.CO;2

Wu, R., Hu, Z.-Z., & Kirtman, B. P. (2003). Evolution of ENSO-Related Rainfall Anomalies in East Asia. *Journal of Climate, 16*(22), 3742-3758. https://doi.org/10.1175/1520-0442(2003)016<3742:EOERAI>2.0.CO;2

Wu, R., Hu, Z.-Z., & Kirtman, B. P. (2003). Evolution of ENSO-Related Rainfall Anomalies in East Asia. *Journal of Climate, 16*(22), 3742-3758. https://doi.org/10.1175/1520-0442(2003)016<3742:EOERAI>2.0.CO;2

Xie, A., Xu, H. M., Xu, H. M., & Ma, J. (2014a). Atmospheric response to the sea surface temperature front of Kuroshio over the East China Sea under different prevailing surface winds in spring. *Journal of the Meteorological Sciences*, 34(4), 355–364. https://doi.org/10.3969/2014jms.0037

Xie, W., Li, N., Li, C., Wu, J.-d., Hu, A., & Hao, X. (2014b). Quantifying cascading effects triggered by disrupted transportation due to the Great 2008 Chinese Ice Storm: implications for disaster risk management. *Natural Hazards, 70*(1), 337-352. https://doi.org/10.1007/s11069-013-0813-9

Xu, G., Chang, P., Ma, X., & Li, M. (2019). Suppression of winter heavy precipitation in Southeastern China by the Kuroshio warm current. *Climate Dynamics, 53*(3), 2437-2450. https://doi.org/10.1007/s00382-019-04873-3

Xu, H., Xu, M., Xie, S.-P., & Wang, Y. (2011). Deep Atmospheric Response to the Spring Kuroshio over the East China Sea. *Journal of Climate, 24*(18), 4959-4972. https://doi.org/10.1175/JCLI-D-10-05034.1

Xu, M., & Xu, H. (2015). Atmospheric Responses to Kuroshio SST Front in the East China Sea under Different Prevailing Winds in Winter and Spring. *Journal of Climate, 28*(8), 3191-3211. https://doi.org/10.1175/JCLI-D-13-00675.1

Yao, Y., Lin, H., & Wu, Q. (2015). Subseasonal Variability of Precipitation in China during Boreal Winter. *Journal of Climate, 28*(16), 6548-6559.

https://doi.org/10.1175/JCLI-D-15-0033.1

Ye, Q. (2014). Building resilient power grids from integrated risk governance perspective: A lesson learned from china's 2008 Ice-Snow Storm disaster. *The European Physical Journal Special Topics, 223*(12), 2439-2449. https://doi.org/10.1140/epjst/e2014-02218-7

Zhou, B., Gu, L., Ding, Y., Shao, L., Wu, Z., Yang, X., . . . Kong, W. (2011). The Great 2008 Chinese Ice Storm: Its Socioeconomic Ecological Impact and Sustainability Lessons Learned. *Bulletin of the American Meteorological Society, 92*(1), 47-60. https://doi.org/10.1175/2010BAMS2857.1

Zhou, B., Wang, X., Cao, Y., Ge, X., Gu, L., & Meng, J. (2017). Damage assessment to subtropical forests following the 2008 Chinese ice storm. *IForest, 10*(2), 406-415. https://doi.org/10.3832/ifor1619-009

Zhou, L.-T., & Wu, R. (2010). Respective impacts of the East Asian winter monsoon and ENSO on winter rainfall in China. *115*(D2). https://doi.org/10.1029/2009JD012502